# Maturity Issues within Palaeocene Coal, Spitsbergen: Implications for local and regional burial and uplift models

Chris Marshall[a*], Jacob Uguna[a], David J. Large[a], Will Meredith[a], Malte Jochmann[b], Bjarki Friis[b], Christopher H. Vane[c], Baruch F. Spiro[d], Colin E. Snape[a], Alv Orheim[e]

[a] *Corresponding Author; Christopher.Marshall@nottingham.ac.uk Department of Chemical and Environmental Engineering, Faculty of Engineering, University of Nottingham, University Park, Nottingham NG7 2RD, UK (0115) 9514114

[b] Store Norske AS, PO Box 613, NO-9171 Longyearbyen, Norway

[c] British Geological Survey, Nicker Hill, Keyworth, Nottingham, NG12 5GG, UK

[d] Department of Mineralogy, Natural History Museum, Cromwell Road, London SW7 5BD, UK

[e] GeoArktis As, Rosestien 3, N-4022 Stavanger, Norway

**The Central Tertiary Basin is an uplifted part of the North Barents Shelf and should be an ideal location to understand the thermal history, maximum burial depth and overburden thickness in this petroleum-rich area. Efforts to quantify the thermal history of the region have been hampered by reports of hyper-thermal conditions, maturity gaps and maturity inversions in the Tertiary vitrinite reflectance ($R_o$) record. This has been attributed to thermal insulation effects, bitumen suppression and later Tertiary volcanism. Through the use of $R_o$, organic maturity parameters, $^{13}C$ NMR and Rock-Eval pyrolysis, this study aims to explain the unusual maturity effects observed and the implications for burial models. Within single seams, $R_o$ % ranges from 0.5-0.78 with increasingly bimodal distribution up-seam. Analysis of coal aromaticity and the results of Rock-Eval analysis confirm that maturity gaps and inversions only occur where the vitrinite reflectance has been suppressed by high bitumen content (300-400 mg/g coal). Samples with the lowest hydrogen index values (<250 mg HC/ TOC) provide the most accurate estimates of the vitrinite reflectance. Results indicate maximum burial temperatures of 120°C in the basin centre and 100°C at the basin margins with a hyper-thermal gradient of approximately 50°C/km. This gradient implies a total overburden of 2 km of which 1 km has been lost. Maximum burial depth and total erosional sediment load to the Barents Shelf are therefore at the lower end of current estimates.**

**Key Words**

Vitrinite Reflectance, Oil prone coal, Maturity, Barent Shelf, Spitsbergen

## 1. Introduction

Apparent maturity gaps and maturity inversions in vitrinite reflectance ($R_o$) data appear common within the Central Tertiary Basin, notably between the Triassic-Jurrassic boundary and Cretaceous-Basal Tertiary strata (Paech and Koch, 2001). Orheim et al. (2007) also report a maturity gap ($R_o$ %=0.94 vs. 0.71) within Basal Tertiary Firkanten Formation coal seams which stratigraphically are only 40 m apart. Tertiary vitrinite reflectance ($R_o$) data forms a key part of many estimates regarding geothermal gradient, maximum burial depth and overburden loss (Major and Nagy, 1972, Manum and Throndsen, 1978, Throndsen, 1982, Paech and Koch, 2001). Any significant suppression of vitrinite may therefore lead to changes to estimates of erosion and transportation to local depocentres such as the Barents Sea,

Orheim et al., (2007) provide two possible explanations for apparent maturity variations within the Tertiary coals, namely the insulation effect of an underlying seam and suppression of vitrinite reflectance by bitumen enrichment. Hyper-thermal conditions during burial have been implied in a number of studies of the Adventdalen Area (Fig. 1; Major and Nagy, 1972, Manum and Throndsen, 1978, Throndsen, 1982, Paech and Koch, 2001, Braathen, 2012). In addition, it is clear that the Central Tertiary Basin was subject to local volcanic activity during the Tertiary as shown by numerous bentonite beds in Van Mijenfjorden Group sediments (Fig. 2), and a dolerite sill in the Bjørndalen/Fuglefjellet region (Pers. Comm. Trygvason Eliassen, 2014). The effect on vitrinite reflectance in the case of intrusions is expected to be significant but highly localised.

Vitrinite suppression by bitumen is well documented in oil source rocks including coals. Fluorescent (perhydrous) vitrinites enriched in hydrogen rich material are an indicator of oil potential and therefore of the potential for suppressed vitrinite reflectance ($R_o$) values (Diessel and Gammidge, 1998). As vitrinite reflectance is an indirect measure of aromaticity (Carr and Williamson, 1990) any excess aliphatic material will lead to $R_o$ values suppression. Orheim et al. (2007) observed that the upper Firkanten formation coals fluoresce under UV light and produce droplets of oil during preparation. In addition, Marshall (2013) show that the coals produce up to 40 wt% hydrocarbons, when processed by Soxhlet solvent extraction and hydrous pyrolysis. This would indicate that the coals have at least some oil potential and therefore bitumen suppression may present a reasonable explanation.

In this study we examine bulk and high resolution vitrinite reflectance measurements to examine whether reported $R_o$ variability can be replicated. We utilise other independent maturity parameters such as organic biomarkers, Rock-Eval and aromaticity to provide an alternative measure of maturity in the coals. Focussing upon the role of oil potential in $R_o$ suppression we compare Rock-Eval hydrogen index (HI) values with vitrinite reflectance to attempt to correct for the suppression effect. The implications for the thermal regime, missing overburden estimates, sediment compaction and sediment transportation to the Barents Sea are then discussed.

## 2. Geological Setting

Svalbard (Fig.1) represents an uplifted part of the Northern Barents shelf (Harland et al., 1997) comprising Caledonian basement and subsequent uncomformable basin infill. Much of central and southern Spitsbergen forms part of the Central Tertiary Basin a asymmetric synclinal basin, bounded to the east and west by the Billefjorden Faultzone and West Spitsbergen fold and thrust belt. Formed in response to the onset of compression related West Spitsbergen foreland fold and thrusting and prior to the strike-slip separation of Svalbard and Barents Shelf from Greenland (Harland, 1997, Tessensohn, 2001) the Central Tertiary Basin contains sediments dating from as early as the Carboniferous including many source rock analogues from the wider Barents sea region. It also contains the majority of the economic coal deposits on the islands, with mining concentrated within the Tertiary Firkanten Formation

In the NE Central Tertiary Basin, the Firkanten Formation comprises two sub-units; the lowermost Todalen Member and the overlying Endalen Member representing a sequence of paralic coalbearing tidal sediments overlain by laminated or heavily bio-turbated marine sandstones (Fig. 2; Dallmann *et al.*, 1999). The base of the Firkanten Formation is marked by a low angle unconformity with the Lower Cretaceous Carolinefjellet formation, sometimes marked by a basal conglomerate known as the Grønfjorden bed (Harland, 1997, Dallmann, 1999).

To the west an additional offshore unit is also observed, known as the Kolthoffberget Member (Fig. 2; Dallmann, 1999). The Todalen Member represents the main coal bearing unit within the Van Mijenfjorden Group and therefore is the focus of this study. It consists of 3-5 siltstone-sandstone-coal successions representing increased subsidence and the infilling of the Cretaceous pene-plain (Harland, 1997, Dallmann, 1999). Five main coal seams are commonly cited within the Todalen Member; the Svea, Todalen, Longyear, Svarteper and Askeladden Seams (Fig. 2; Dallmann, 1999, Harland, 1997, Orheim et al., 2007)).

## 3. Methodology

Coal was sampled (Fig. 1) from the Svea Nord, Longyear and Svarteper seams from mine sections in Svea Nord and Mine 7, boreholes from the Lunckefjellet (BH6A-2007, BH10/2007, BH10/2009, BH15/2011), Adventdalen (BH4/2009, BH5/2009) and Colesdalen (BH3/2008) regions, and a field section from Bassen. Samples were coarse-crushed, separated by cone and quarter (to allow unbiased sampling for coal maceral analysis) and the remainder fine crushed (<100 μm). Polished blocks (particle size; 0.2 – 1 mm) were created for organic petrology and vitrinite reflectance ($R_o$).

Coal vitrinite reflectance ($R_o$) was determined using a microscope fitted with a 50x oil immersion objective and 10x oculars, 12 V 100 W quartz halogen lamp and 100 W HBO high pressure mercury lamp. $R_o$ measurements were taken using an attached photomultiplier (100 points) and calibrated using a 1.24 $R_o$, 564 nm glass prisma standard and blank plastic oil-filled depression according to BSI standards (British Standard Institution, 2009).

To determine the amount of hydrocarbon potential the coals were analysed using a Rock-Eval6 analyser configured in standard mode (pyrolysis and oxidation as a serial process) to indicate the coals (20 mg dry wt) were heated from 300ºC to 650ºC at 25ºC/min in an inert atmosphere of $N_2$ and the residual carbon then oxidised at 300ºC to 850ºC at 20ºC/min (hold 5 min). Hydrocarbons released during the two stage pyrolysis were measured using a flame ionization detector and CO and $CO_2$ measured using an IR cell. The performance of the instrument was checked every 10 samples against the accepted values of the Institut Français du Pétrole (IFP) standard (IFP 160 000, S/N1 5-081840). Classical Rock-Eval parameters were calculated by integration of the amounts of HC (thermo-vaporized free hydrocarbons) expressed in mg/HC/g rock ($S_1$) and hydrocarbons released from cracking of bound OM expressed in mg/HC/g rock ($S_2$)

(Engelhart et al., 2013). The Hydrogen Index (HI) was calculated from $S_2$ x 100/TOC and the Oxygen Index (OI), $S_3$ x 100/TOC. The error on the $T_{max}$ is about ±6 °C.

In order to examine organic maturity parameters in the solvent extractable hydrocarbon fraction from the Adventdalen coals (BH-5-2009 and Mine 7 Section), the coals were subjected to accelerated solvent extraction (ASE) using a 93:7 DCM: methanol mixture for a period of 24hrs, and separated into aliphatic, aromatic and polar fractions by silica-alumina adsorption column chromatography (15 ml *n*-hexane; 15 ml *n*-hexane:DCM (3:2 v/v); 15 ml DCM:,methanol (1:1 v/v). Aliphatic and aromatic fractions were analysed by GC-MS in both the SIM and full scan (m/z 50-450) modes, using a Varian CP-3800 gas chromatograph, interfaced to a Varian 1200 mass spectrometer (EI mode, 70eV). Seperation was achieved on a VF-1MS fused silica capillary column (50m x 0.32 mm i.d, 0.25 µm stationary phase thickness), with helium as the carrier gas, and an oven programme of 50°C (hold for 2 min) to 300°C (hold for 20.5 min) at a heating rate of 4°C/min. The $m/z$ 85 single ion chromatogram (SIC) was used to measure *n*-alkane peak area response. Relative hopane and sterane concentrations were from peak area responses in the $m/z$ 191 and $m/z$ 217 SICs, respectively. MPI-1 was calculated from the aromatic fraction from peak area responses from the $m/z$ 178 and $m/z$ 192 SICs respectively (after Cassani et al., 1988).

The ratio of aliphatic to aromatic components was determined in selected Svea Nord and Longyear coal samples (1.20 m and 1.30 m above seam base respectively) using high resolution solid state 50 MHz $^{13}C$ NMR. Analysis was carried out in a BrukerAvance 200 spectrometer to ascertain using the cross polarisation (CP) sequence in conjunction with magic angle spinning (MAS). For CP-MAS analysis, the acquisition time was 0.05 s, the relaxation delay was 1.5 s and the contact time was 1 ms. Samples were packed tight into a cylindrical (7 mm o.d.) zirconia rotor with a cap made of a homopolymer of chlorotrifluoroethene (Kel-F) and spun at the magic angle (54.74°) with a spinning rate of approximately 5 kHz. Tetrakis-trimethylsilyl) silane (TKS) was added to the samples as an internal standard. The number of scans was 2500 and the free induction decays (FIDs) were processed using a line broadening factor of 50 Hz.

## 4. Results

### 4.1 Vitrinite Reflectance

Examination of vitrinite reflectance values (Table 1) from two bulk samples of Svea and Longyear coal examined replicate the maturity gap reported by Orheim et al. (2007) with $R_o$ % values of 0.65 vs 0.78. Consequently, to understand how widespread and the main cause of this difference in maturity the Longyear seam was examined at higher resolution in coals from three sub-regions; Adventdalen, Lunckefjellet and Colesdalen.

### 4.2 Adventdalen

Coals from the Adventdalen region are vitrinite dominated with low inertinite and liptinite with the exception of the Svea seam which is inertinite dominated. Vitrinites are observed to exhibit dull orange/brown fluorescence under blue light. $R_o$ values range from 0.5-0.8 with the Svea seam showing generally highest values and uppermost Longyear seam the lowest (Fig 3; Table S1). All sites show a similar range of $R_o$ values which is unexpected as the Bassen section is up-dip of samples from Breinosa area. The distribution of $R_0$ values exhibits the greatest range in Mine 7 and Bassen samples with minimum values at Mine 7 of 0.5. There are distinct differences between upper and lower seams in Mine 7 and Bassen section. These numerous small and large scale variations comprising rapid $R_o$ drops and inversions are unlikely to be the product of differing thermal histories. Conversely $R_o$ values from the BH4/2009 sample locality remain consistently low, which is perhaps the product of a more homogenous composition.

When the distribution of $R_o$ data in the Mine 7 section is examined in greater detail it indicates a general broadening of $R_o$ measurements up-seam (Fig. 4) accompanied by a gradual reduction in the number of higher reflectance measurements. In addition rather than a single main peak, measurements become increasingly bimodal up-seam. This bi-modality is possibly the product of variation in the relative number of fluorescent vs. non-fluorescent vitrinites.

### 4.3 Lunckefjellet

The Lunckefjellet Longyear seam is vitrinite dominated (as in Adventdalen) with low inertinite and liptinite. Vitrinites again exhibit dull orange/brown fluoresce under blue light. Highest vitrinite reflectance values (≈0.76) are found towards the eastern margin of the basin (Fig 5; Table S1) with decreasing $R_o$ down dip which is contrary to expectations. In addition the Longyear seams exhibit a general decrease in $R_o$ up-seam similar to that seen in Adventdalen. The greatest range of $R_o$ values (Fig. 5) can be found in the easternmost sampling locality's with values ranging from $R_o$ % 0.59-0.76. These numerous small and large scale variations comprising rapid $R_o$ drops and inversions are unlikely to be the product of differing thermal histories. As in Adventdalen, when the distribution of $R_o$ data in the Lunckefjellet section (Fig. 6) is examined in greater detail it indicates a general broadening of $R_o$ measurements up-seam (Fig 6). In addition measurements become increasingly bimodal up-seam. The high degree of similarity between the Adventdalen and Lunckefjellet coals indicates that a similar process is controlling the large variations in vitrinite reflectance at both sites.

### 4.4 Colesdalen

The Colesdalen coals are higher in inertinite (compared to the other coals in this study) but still vitrinite dominated. The Colesdalen coals have elevated $R_o$ values (0.78) as expected from a more central part of basin (Table S1). In addition the Colesdalen coals show less variability with values consistently high throughout the seam with the exception of two more ash rich samples.

The vitrinite reflectance measurements (Table S1) from the Lunckefjellet and Adventdalen regions show large variations ($R_o$ % ≈ 0.3) within some parts of the seam and importantly replicate the maturity gap observed (Orheim et al., 2007). These numerous small and large scale variations comprising rapid $R_o$ drops and inversions are unlikely to be the product of differing thermal histories. As a result, the suitability of vitrinite reflectance in these coals as a measure of maturity will be examined by comparing $R_o$ data with independent measures of maturity such as organic maturity parameters, Rock-Eval and aromaticity.

### 4.5 Organic Maturity parameters

Coals from BH 5/2009 and Mine 7 were selected to further examine the true maturity of the Svea, Longyear and Svarteper seams through organic geochemical biomarkers in Soxhlet extracted oils. Organic Geochemical maturity parameters (Table 1) can be highly specific at low maturities but often reach equilibrium at around $R_o$ 0.7%, making many of little use at higher maturities (Peters et al., 2005).

Aliphatic maturity parameters for the Todalen coals are at or approaching equilibrium (Table. 1) indicating a maturity in excess of $R_o$ 0.7%. The *n*-alkanes show little odd over even predominance, with carbon preference index values (CPI(1),(Bray and Evans, 1961)) close to mature ratios (≈1). Notably, both CPI(1), sterane and hopane maturity parameters shown no change up-seam in the Longyear (Fig.7) contrary to what would be expected if $R_o$ values at the top of the seam represented true maturity values and were not suppressed.

Consideration of the aromatic Methylphenanthrene Index, MPI-1 (Radke et al., 1982, Radke et al., 1986, Radke, 1988) predicts $R_o$ values of around 0.72±0.05 in the Svea, Longyear and Svarteper seams in the Adventdalen region with no changes up-seam (Table 1). Although the predicted values are lower than maximum $R_o$ values measured in these coals ($R_o$% ≈ 0.78), the predicted values remain substantially higher than the lowest values measured at the top of the Longyear seam in Mine 7 ($R_o$ % ≈ 0.5). A possible explanation for the difference is the effect of variation in organic matter source and migration (Peters et al., 2005). Differences between predicted MPI-1 $R_o$ % (0.72) and measured $R_o$ (0.79) in the Svea seam at both Adventdalen and Svea Nord are likely a product of differing palaeo-environment and associated organic matter.

In summary, geochemical evidence points to both seams having comparable maturities and thermal histories. Significantly, the $R_o$ maturity gap, both within the Longyear seam and between the Svea and Longyear seams is not reproduced geochemically.

### 4.6 Oil Potential and Maturity

$T_{max}$, like many maturity parameters is highly dependent upon source material (Peters et al., 2005) but is considered of use for assessment of Type II material (420-460°C) and Type III (400-600°C; Tissot et al., 1987). $T_{max}$ ranges from 425–448°C for all the Svalbard coals indicating a maximum maturity in the early-mid oil window (Table. S2). When $T_{max}$ is plotted against HI (indicative of source rock potential; Fig. 8) there is a general positive correlation with coal from the basin margin at Lunckefjellet and Bassen least mature and Colesdalen coals from the basin centre more mature. HI also appears to peak within the coals between $T_{max}$ values between 435 and 445°C. This is similar to the $HI_{max}$ concept, and is associated with the reorganisation of kerogen structure (Petersen, 2005).

When $T_{max}$ is converted to $R_o$ (Teichmüller and Durand, 1983) values were elevated compared to measured values indicating thermal maturity $R_o$ % ≈0.83 (Table S2) for all samples in the Adventdalen region with the exception of Bassen where the more marginal basin setting means the coals are inherently less mature. Coals from the Svea Nord seam are slightly more mature than those in Adventdalen, consistent with the southward tilting of the Central Tertiary Basin. The Svea Nord seam has values around 0.85. The Lunckefjellet coals appear less mature than the Svea Nord and Adventdalen coals with calculated $R_o$ % values of 0.66, perhaps consistent with a more marginal setting. The Colesdalen coals as expected due to their more central location are more mature with calculated $R_o$ % values of 0.83.

The production index ($PI = S_1/(S_1+S_2)$) is another indicator of maturity values, < 0.1 indicate an immature source rock and values > 0.4, a mature source rock (Maky and Ramadan, 2008). The Svalbard coals all have values <0.1 (Table. S2; Fig 8), suggesting the coals were exhumed prior to any significant generation of hydrocarbons, with Colesdalen the most mature with values approaching 0.1 (Fig.8). As with $T_{max}$ the coals with the highest HI values appear to be closest to generation, particularly in the Colesdalen region (Fig.8). The Bassen region appears to have unusually low free hydrocarbon values which may reflect weathering at the field site. Values of $T_{max}$ appear slightly high compared to PI values which indicate that the coals are sub-mature. This may be due to the extended oil window in coals compared to other conventional source rocks (Petersen and Nytoft, 2006).

HI values in the Svea seam are generally <250mg HC/TOC with upper seams ranging between 250-400 mg HC/TOC (Table S2). This confirms that the upper coal seams across eastern central basin have significant oil potential compared to the Svea Seam. The plot of HI vs OI (Fig.8) shows that most samples have compositions between that of Type II and Type III kerogen. OI is elevated and HI lower in the Bassen area indicates either lower maturity or weathering of samples. As this is a field sample and the vitrinite reflectance variations are similar to other sample locations in the area it is thought most likely to indicate weathering.

Examination of the relationship between HI and $R_o$ (Fig.8) shows that all sites show strong negative correlation between $R_o$ and HI indicating that the higher the oil potential the more suppressed vitrinite becomes. However the different gradients and positions of these lines show that this relationship is complicated by other factors. These are likely to be compositional, positional and weathering effects. This indicates that samples with the lowest HI values provide a better reflection of the degree of coalification (≈$R_o$ % 0.78-0.80). This fits better with the production and migration of hydrocarbons described previously (Orheim et al., 2007, Marshall, 2013). Consequently, bitumen must have a suppressing effect on $R_o$ across the basin.

### 4.7 Quantifying the suppression effect

Direct measurement of aromaticity (of which $R_o$ is an indirect measurement) is a useful tool in the derivation of maturity in some coals (Stephens et al., 1985, Carr and Williamson, 1990).

The aromaticity (%) of the Svalbard coals (Fig.9) differs greatly between the Longyear and Svea seams (50% vs. 70% respectively). Using the calibration of Carr and Williamson, (1990), yields equivalent $R_o$ values of 0.76 % (Svea) and 0.50% (Longyear). This is clearly not the case, as the Longyear seam bears no resemblance to a brown coal and is likely to have entered the early oil window in most areas. The Svea, which is not oil prone, exhibits an aromaticity consistent with observed maturity. Consequently, the observed maturity gap between the Svea and Longyear seams must be caused by significant amounts of additional aliphatic material within the Longyear seam.

To quantify this suppression effect from normal bituminous Svea coal (75 parts aromatic: 25 parts aliphatic), additional aliphatic carbon within the oil prone Longyear coal would account for 33% of total carbon. This is approximately equivalent to 380-400mg/g TOC, which is very close to HI values observed throughout the Eastern Central Tertiary Basin (Table S2). Variations in the amount of additional aliphatic material must therefore be responsible for apparent inter and intra seam maturity variation, maturity gaps and maturity inversions within Firkanten Formation coals.

## 5. Discussion

### 5.1 Maturity of coals

At a bulk scale the $R_o$ difference observed (Orheim et al., 2007) has been replicated with the Longyear seam in particular appearing to show a rapid decrease in maturity up-seam. However, this variability does not appear to be replicated by independent measures of maturity such as organic maturity parameters and Rock-Eval. In addition these parameters indicate that the coals have a thermal maturity in excess of $R_o$ % 0.70 indicating that the coals reached maturities consistent with the early to mid oil window.

The bulk sample from the Longyear coal contains around 30% extra aliphatic material compared to the Svea seam. This is likely to reflect enrichment in bitumen. This liquid hydrocarbon potential is seen throughout the localities with Rock-Eval HI values ranging from 250-400mg HC/TOC. This is consistent with observed oil production (Orheim et al., 2007) and total hydrocarbon yields from Rock-Eval (300-400 mg HC/TOC) and Soxhlet/hydrous pyrolysis (300-400 mg/g HC; Marshall, 2013).

The effect upon $R_o$ is clear (Fig.8) showing the higher HI values are the more suppressed $R_o$ values become. This vitrinite suppression effect by the enrichment of later seams in aliphatic rich bitumen compared to non-oil prone Svea seams is therefore considered the primary cause for the maturity gaps and inversions observed by Orheim et al., (1997) (Orheim et al., 2007). Consequently, earlier Carboniferous, Jurassic and Cretaceous coals in the basin with observed coal rank inversion and maturity gaps (Paech and Koch, 2001) may benefit from further examination of this effect. The most accurate values for the Longyear seam appear to be found at the base of the seam which would give thermal maturities of the coals of $R_o$ % of 0.78 at Breinosa, 0.68 at Bassen, 0.76 at Lunckefjellet and 0.80 in the Colesdalen area.

**5.2 Thermal regime and implications for overburden models**

Previous models measuring coalification gradients in Tertiary strata from the Adventdalen area range from between 0.17-0.32% $R_o$/km (Paech and Koch, 2001 and references therein). However due to the bitumen suppression effect it is likely that $R_o$ values lie somewhat higher than previously thought. As the highest values of $R_o$ in each seam appear the most reliable the maximum overburden and thermal regime at peak burial was calculated using these values and the empirical palaeo-temperature equation (Barker and Pawlewicz, 1994);

$$\text{Max T } (°\text{C}) = \frac{\text{Ln}(\text{Ro}) + 1.68}{0.0124}$$

$R_o$ values indicate estimated peak temps of 116°C in the Colesdalen area, 111°C at Breinosa, 110°C at Lunckefjellet and 100°C at Bassen. As expected, coals from the centre of the basin were exposed to the highest temperatures and vice versa. Given normal continental geothermal gradients (25°C/km) and assuming no other heat sources (Corcoran and Clayton, 1999) this would reflect maximum burial depths of 4.6 km, 4.4 km, 4.4 km and 4.0 km respectively. In the Adventdalen area this would equate to a total missing overburden of 3.4 km which is much greater than other estimates from the Central basin (Paech and Koch, 2001 and references therein).

Assuming reported $R_o$ values of 0.43 for the upper Tertiary coals from the Aspelintoppen Formation are correct (Throndsen, 1982) and values for the stratigraphically lower Firkanten Formation coals 0.78 then the Ro gradient will be 0.35 $R_o$/km. This is consistent with the highest previous estimates (Paech and Koch, 2001). When converted using the Barker and Pawlewicz, 1994 equation this equates to a geothermal gradient of around 50°C/km, similar to previous estimates (40°C/km; Braathen et al., 2012) and maximum burial depths of 2.3km in the Colesdalen area, 2.2km at Breinosa, 2.2 km at Lunckefjellet and 2.0 km at Bassen. As approximately 1.0 km of overlying strata still exists in the Adventdalen Region (Throndsen, 1982) the missing overburden is likely to amount to ~1.0 km. This is lower than the values of 1.7km previously reported (Paech and Koch, 2001 and references therein). In more central and southern areas of the basin, accounting for vitrinite suppression, would also greatly reduce the current estimated 3 km of eroded overburden (Manum and Throndsen, 1978).

Previous studies support the conclusion (Major and Nagy, 1972, Manum and Throndsen, 1978, Throndsen, 1982, Paech and Koch, 2001) that the geothermal gradient during burial was hyper-thermal. This is unsurprising as the Central Tertiary Basin was formed during a period of both local and regional tectonic activity. Additionally the presence of a dolerite sill in the Bjørndalen area (Pers. Comm. Trygvason Eliassen, 2014) and the numerous volcanic bentonites within Tertiary strata indicate volcanism played an important role in shaping the thermal history of the Central Tertiary Basin. Hyper-thermal conditions may also explain the relatively low levels of compaction observed in Tertiary strata when compared to their apparent maturity.

Within a regional context, the Northern Barents including Svalbard (regarded as an uplifted NW edge of the Barents Shelf, Harland, 1997) was subjected to less burial and subsequent uplift and erosion than previously thought (Manum and Throndsen, 1978, Throndsen, 1982, Paech and Koch, 2001) and consequently fits with lower estimates of erosion and sediment load to the Southern Barents during the late Cenozoic (Rasmussen and Fjeldskaar, 1996).

## 6. Conclusions

Inferred maturity gaps within the Svalbard coal are shown to be due to suppression of vitrinite reflectance by bitumen enrichment. Upper Firkanten formation coals have significant oil potential (HI 250-400mg HC/TOC), they appear most affected by maturity issues, displaying considerable variability in $R_o$ values. Only the lowermost (and least oil prone) parts of the coal seams remain relatively unaffected. Using these values for the Adventdalen region, indicates $R_o$ % values ranging from 0.68 at the basin margin to 0.78 4 km down-dip, At Lunckefjellet $R_o$ % values are around 0.76 and in the more centrally located Colesdalen values of 0.80. Coalification gradients in Adventdalen equate to ~0.35 $R_o$/km consistent with highest previous estimates (Paech and Koch, 2001), a thermal gradient of approximately 50°C/km and peak burial depths of ~2km in the Adventdalen region. This indicates overall overburden erosion was less than previous estimates (1.7km; Manum and Throndsen, 1978) at around 1.0 km. The results of this study indicate that burial and subsequent uplift and erosion were perhaps lower than previously thought, leading to less compaction of tertiary strata on Svalbard and resulting in reduced sediment load to the Barents Shelf in the Late Tertiary.

## Acknowledgements

We wish to thank Statoil & Store Norske AS for providing the samples used in this study. Many thanks also to Mr. David Clift for assistance with maceral analysis and sample preparation, Prof. Trevor Drage for assistance with NMR and Prof. Snorre Olaussen and the University Centre on Svalbard for helpful discussions and logistical support. Financial Support by Store Norske AS/University of Nottingham studentship and NERC Studentship is gratefully acknowledged.

## References

BARKER, C., E. & PAWLEWICZ, M., J. 1994. Calculation of Vitrinite Reflectance from Thermal Histories and Peak Temperatures. *Vitrinite Reflectance as a Maturity Parameter*. American Chemical Society.

BRAATHEN, A., BÆLUM, K., CHRISTIANSEN, H. H., DAHL, T., EIKEN, O., ELVEBAKK, H., HANSEN, F., HANSSEN, T. H., JOCHMANN, M., JOHANSEN, T. A., JOHNSEN, H., LARSEN, L., LIE, T., MERTES, J., MØRK, A., MØRK, M. B., NEMEC, W., OLAUSSEN, S., OYE, V., RØD, K., TITLESTAD, G. O., TVERANGER, J. & VAGLE, K. 2012. The Longyearbyen CO2 Lab of Svalbard, Norway - initial assessment of the geological conditions for CO2 sequestration. *Norwegian Journal of Geology*, 92, 353-976.

BRAY, E. E. & EVANS, E. D. 1961. DISTRIBUTION OF NORMAL-PARAFFINS AS A CLUE TO RECOGNITION OF SOURCE BEDS. *Geochimica Et Cosmochimica Acta,* 22**,** 2-15.

BRAY, R. J., GREEN, P. F. & DUDDY, I. R. 1992. Thermal history reconstruction using apatite fission track analysis and vitrinite reflectance: a case study from the UK East Midlands and southern North Sea. *In:* HARDMAN, R. F. P. (ed.) *Exploration Britain: geological insights for the next decade.* London: Geological Society of London.

BRITISH STANDARD INSTITUTION 2009. BS ISO 7404-5:2009: Methods for the petrographic analysis of coals –Part 5: Method of determining microscopically the reflectance of vitrinite. London: British Standard Instiution.

CARR, A. D. & WILLIAMSON, J. E. 1990. THE RELATIONSHIP BETWEEN AROMATICITY, VITRINITE REFLECTANCE AND MACERAL COMPOSITION OF COALS - IMPLICATIONS FOR THE USE OF VITRINITE REFLECTANCE AS A MATURATION PARAMETER. *Organic Geochemistry,* 16**,** 313-323.

CASSANI, F., GALLANGO, O., TALUKDAR, S., VALLEJOS, C. & EHRMANN, U. 1988. Methylphenanthrene maturity index of marine source rock extracts and crude oils from the Maracaibo Basin. *Organic Geochemistry,* 13**,** 73-80.

CORCORAN, D. & CLAYTON, G. 1999. INTERPRETATION OF VITRINITE REFLECTANCE PROFILES IN THE CENTRAL IRISH SEA AREA: IMPLICATIONS FOR THE TIMING OF ORGANIC MATURATION. *Journal of Petroleum Geology,* 22**,** 261-286.

DALLMANN, W. K. 1999. *Lithostratigraphic Lexicon of Svalbard,* Tromsø, Norsk Polarinstitutt.

DIESSEL, C. F. K. & GAMMIDGE, L. 1998. Isometamorphic variations in the reflectance and fluorescence of vitrinite—a key to depositional environment. *International Journal of Coal Geology,* 36**,** 167-222.

ENGELHART, S. E., HORTON, B. P., NELSON, A. R., HAWKES, A. D., WITTER, R. C., WANG, K., WANG, P.-L. & VANE, C. H. 2013. Testing the use of microfossils to reconstruct great earthquakes at Cascadia. *Geology*.

HARLAND, W. B. 1997. Chapter 20 Paleogene history. *In:* HARLAND, W. B. (ed.) *Geological Society, London, Memoirs.* London: Geological Society, London.

HELLAND-HANSEN, W. 1992. Geometry and facies of Tertiary clinothems, Spitsbergen. Sedimentology, 39, 1013-1029.

MAJOR, H. & NAGY, J. 1972. *Geology of the Adventdalen map area,* Oslo, Norsk Polarinstitutt.

MAKY, A. B. F. & RAMADAN, M. A. M. 2008. Nature of Organic Matter, Thermal Maturation and Hydrocarbon Potentiality of
Khatatba Formation at East Abu-gharadig Basin, North Western Desert, Egypt. *Australian Journal of Basic and Applied Sciences,* 2**,** 194-209.

MANUM, S. B. & THRONDSEN, T. 1978. Rank of coal and dispersed organic matter and its geological
bearing in the Spitsbergen Tertiary. *Norsk Polarinstitutt. Arbok.* Oslo.

MARSHALL, C. J. 2013. *Palaeogeographic development and economic potential of the coal-bearing palaeocene Todalen Member, Spitsbergen.* Thesis (Ph.D.), University of Nottingham.

ORHEIM, A., BIEG, G., BREKKE, T., HORSEIDE, V. & STENVOLD, J. 2007. Petrography and geochemical affinities of Spitsbergen Paleocene coals, Norway. *International Journal of Coal Geology,* 70**,** 116-136.

PAECH, H.-J. & KOCH, J. 2001. Coalification in Post-Caledonian Sediments on Spitsbergen. *In:* TESSENSOHN, F. (ed.) *Intra-Continental Fold Belts CASE 1: West Spitsbergen.* Hannover: Geologisches Jahrbuch.

PETERS, K. E., WALTERS, C. C. & MOLDOWAN, J. M. 2005. *The Biomarker Guide Volume 2: Biomarkers and Isotopes in Petroleum Exploration and Earth History. Second Edition.,* Cambridge, Cambridge University Press.
PETERSEN, H. I. 2005. Oil Generation from coal source rocks: the influence of depositional conditions and stratigraphic age. *Geological Survey of Denmark and Greenland Bulletin,* 7**,** 9-12.
PETERSEN, H. I. & NYTOFT, H. P. 2006. Oil generation capacity of coals as a function of coal age and aliphatic structure. *Organic Geochemistry,* 37**,** 558-583.
RADKE, M. 1988. Application of aromatic compounds as maturity indicators in source rocks and crude oils. *Marine and Petroleum Geology,* 5**,** 224-236.
RADKE, M., WELTE, D. H. & WILLSCH, H. 1982. Geochemical study on a well in the Western Canada Basin: relation of the aromatic distribution pattern to maturity of organic matter. *Geochimica et Cosmochimica Acta,* 46**,** 1-10.
RADKE, M., WELTE, D. H. & WILLSCH, H. 1986. Maturity parameters based on aromatic hydrocarbons: Influence of the organic matter type. *Organic Geochemistry,* 10**,** 51-63.
RASMUSSEN, E. & FJELDSKAAR, W. 1996. Quantification of the Pliocene-Pleistocene erosion of the Barents Sea from present-day bathymetry. *Global and Planetary Change,* 12**,** 119-133.
STEPHENS, J. F., LEOW, H. M., GILBERT, T. D. & PHILP, R. P. 1985. Investigation of the relationship between coal maturity and aromaticity: Characteristics of sodium dichromate oxidation products of Australian vitrinite concentrates. *Fuel,* 64**,** 1537-1541.
TEICHMÜLLER, M. & DURAND, B. 1983. Fluorescence microscopical rank studies on liptinites and vitrinites in peat and coals, and comparison with results of the rock-eval pyrolysis. *International Journal of Coal Geology,* 2**,** 197-230.
TESSENSOHN, F. 2001. *Intra-Continental Fold Belts CASE 1: West Spitsbergen,* Hanover, Geologisches Jahrbuch.
THRONDSEN, T. 1982. VITRINITE REFLECTANCE STUDIES OF COALS AND DISPERSED ORGANIC MATTER IN TERTIARY DEPOSITS IN THE ADVENT-DALEN AREA, SVALBARD. *Polar Research,* 1982**,** 77-91.
TISSOT, B. P., PELET, R. & UNGERER, P. 1987. Thermal history of sedimentary basins, maturation indices, and kinetics of oil and gas generation. *AAPG Bulletin,* 71**,** 1445-1466.
TRYGVASON ELIASSEN, G. 2014. *RE: Fieldwork Observations.* Type to MARSHALL, C.

## Figure and Table Captions

**All figures meant for colour online only**

**Table 1** – Vitrinite Reflectance ($R_o$), *n*-alkane, hopane, sterane and aromatic biomarker and maturity parameters within the Central Tertiary Basin coals. [a] *after* Cassani *et al.,* (1988), [b] *after* Radke et al., (1982) *Pr/Ph –pristane/phytane, Pr/nC17 = Pristane/heptadecane ratio, CPI(1)= 2($C_{23}$+$C_{25}$+$C_{27}$+$C_{29}$/ ($C_{22}$+2($C_{24}$+$C_{26}$+$C_{28}$)+$C_{30}$), TS/TM=17a-22,29,30-trisnorhopane/18a-22,29,30-trisnorhopane, TS/TH= Total hopanes/Total steranes*

**Table S1** –Vitrinite Reflectance ($R_o$) values and location for all sites used in this study

**Table S2** – Rock-Eval Pyrolysis results for all sites used in this study. $T_{max}$ conversion to predicted $R_o$ *after Teichmüller and Durand, 1983* and max burial depth calculated from vitrinite reflectance data *after Barker and Pawlewicz, 1994*

**Figure 1** – Map of the island of Spitsbergen showing the mines and settlements of the NW Central Tertiary Basin and sample locality and type.

**Figure 2** – The Van Mijenfjorden Group representing sedimentary infill of the Central Tertiary Basin, modified from Helland-Hansen (1992)

**Figure 3** – Comparison of the vitrintie reflectance profile in the Longyear Seam across Adventdalen from (A) BH4/2009 (B) Mine 7 Section (C) Bassen Field Section. Note the large variations seen in rank and the general trend to lower $R_o$ % values upseam

**Figure 4** – Variation in rank ($R_0$) within the Longyear seam in Mine 7, Adventdalen. Examination of the distribution of vitrinite reflectance values measured shows a shift to lower values, bi-modal distribution upseam.

**Figure 5** – Comparison of the vitrintie reflectance profile in the Longyear Seam across Lunckefjellet from (A) BH 6A/2007 (B) BH 10/2007 (C) BH 15/2011 (D) BH 10/2009. Note the large variations seen in rank and the general trend to lower $R_o$ % values upseam

**Figure 6** – Variation in rank ($R_0$) within the Longyear seam in BH15-2011, Lunckefjellet. As in Adventdalen examination of the distribution of vitrinite reflectance values measured shows a shift to lower values, bi-modal distribution upseam.

**Figure 7** – Variation in hopane and *n*-alkane maturity parameters up-seam within the Longyear seam. Note little variation in maturity up-seam indicating no maturity gap.

**Figure 8** – Rock-Eval data from the Svalbard coals shows (A) HI vs $R_o$ % shows that HI (oil potential exerts a strong control upon vitrinite reflectance in all areas studied N.B ash rich samples were removed as not representative and Lunckefjellet sample represents BH15/2011. (B) HI vs OI shows that the composition of the

Svalbard coals is a cross between Type II and Type III kerogen with the exception of Bassen Samples which has elevated OI values likely due to weathering effects. (C) HI vs $T_{max}$ and (D) HI vs. PI show that the Colesdalen coals are most mature and closest to hydrocarbon generation with the least mature coals found at Bassen. This is expected as Colesdalen is located in a more central basinal position than Bassen at the basin margins.

**Figure 9** – Measurement of aromaticity of the Svalbard Coals of by $^{13}C$ NMR (A) Longyear seam and (B) Svea seam. Note the large difference between the seam indicating an apparent maturity equivalent to that of R0 0.5% and 0.78% respectively (Carr and Williamson, 1990). This cannot be the case as the Longyear is not a lignite, therefore the Longyear is enriched with non-coaly aliphatics.

**Figure 1**

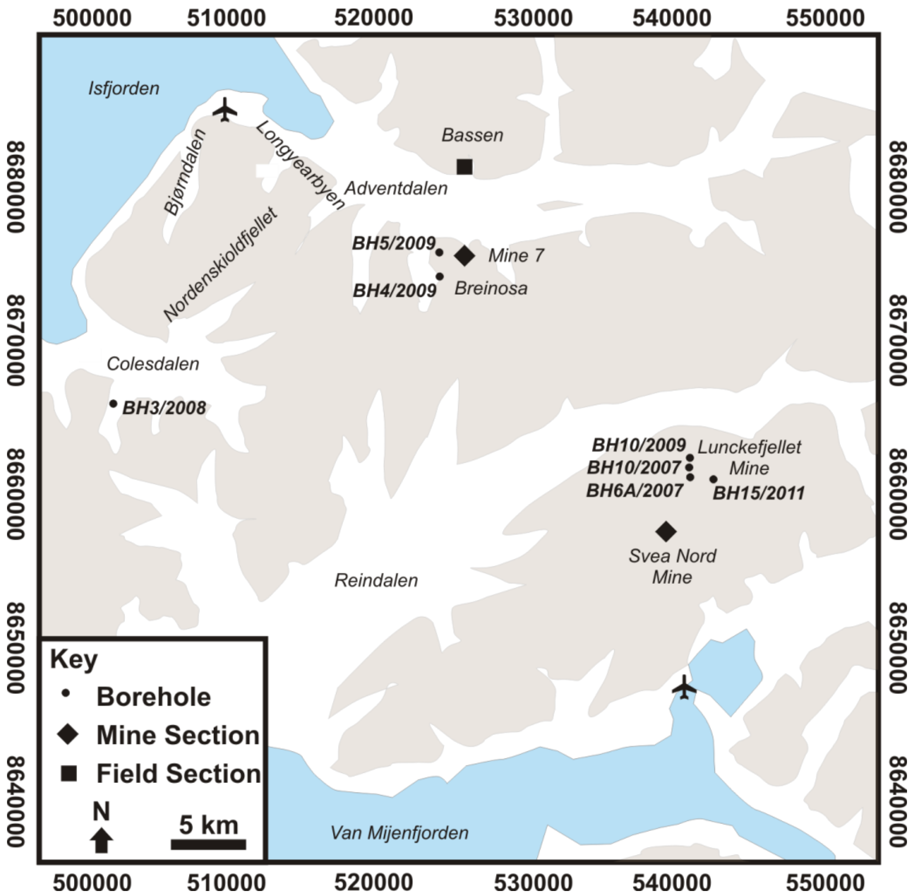
500000
510000
520000
530000
540000
550000
8680000
8670000
8660000
8650000
8640000
Isfjorden
Bjørndalen
Longyearbyen
Bassen
Adventdalen
Nordenskioldfjellet
BH5/2009
Mine 7
BH4/2009
Breinosa
Colesdalen
BH3/2008
BH10/2009
Lunckefjellet
BH10/2007
Mine
BH6A/2007
BH15/2011
Svea Nord
Mine
Reindalen
Van Mijenfjorden
Key
Borehole
Mine Section
Field Section
N
5 km

**Figure 2**

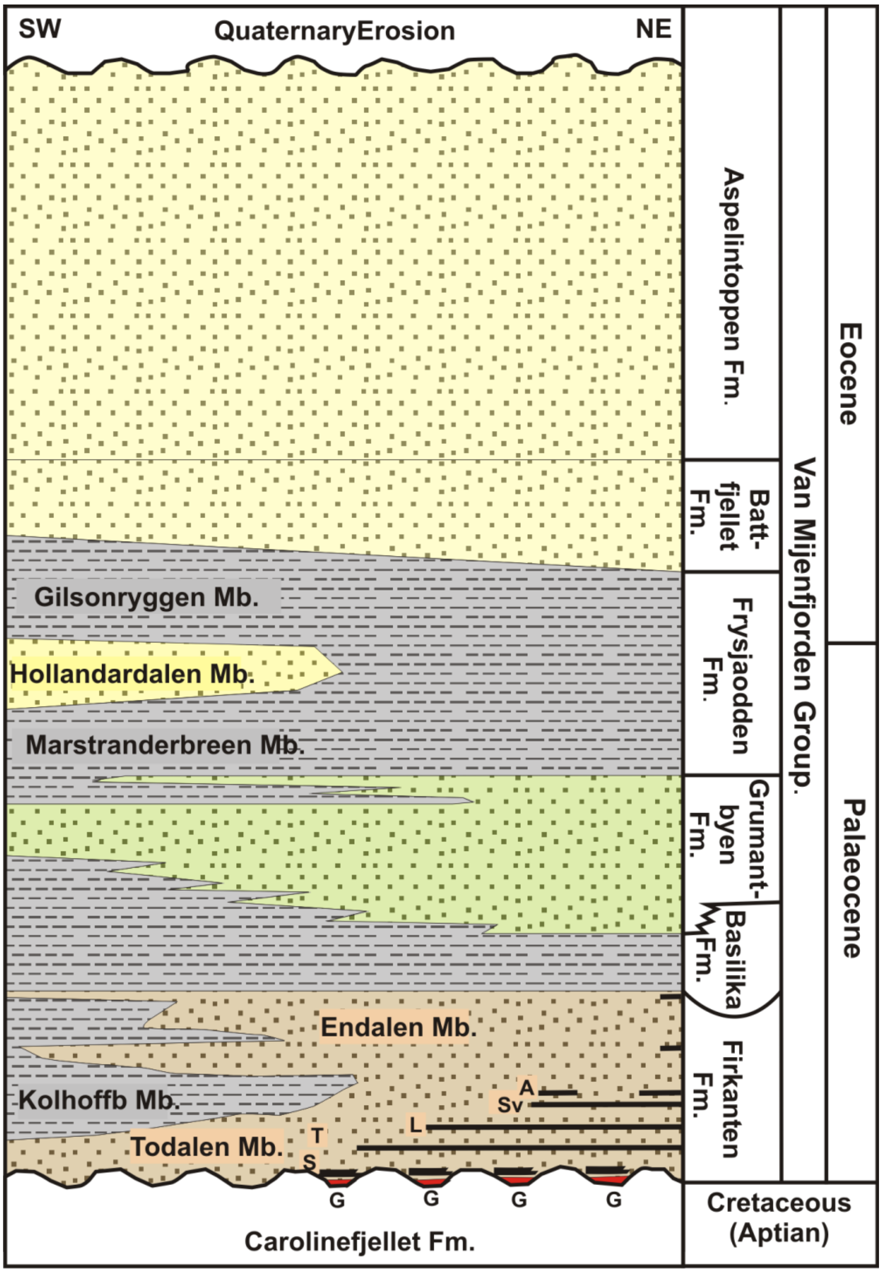
SW
QuaternaryErosion
NE
Aspelintoppen Fm.
Batt-
fjellet
Fm.
Gilsonryggen Mb.
Hollandardalen Mb.
Frysjaodden
Fm.
Marstranderbreen Mb.
Grumant-
byen
Fm.
Basilika
Fm.
Endalen Mb.
Kolhoffb Mb.
Todalen Mb.
Firkanten
Fm.
A
Sv
L
T
S
G
G
G
G
Carolinefjellet Fm.
Van Mijenfjorden Group.
Eocene
Palaeocene
Cretaceous
(Aptian)

**Figure 3**

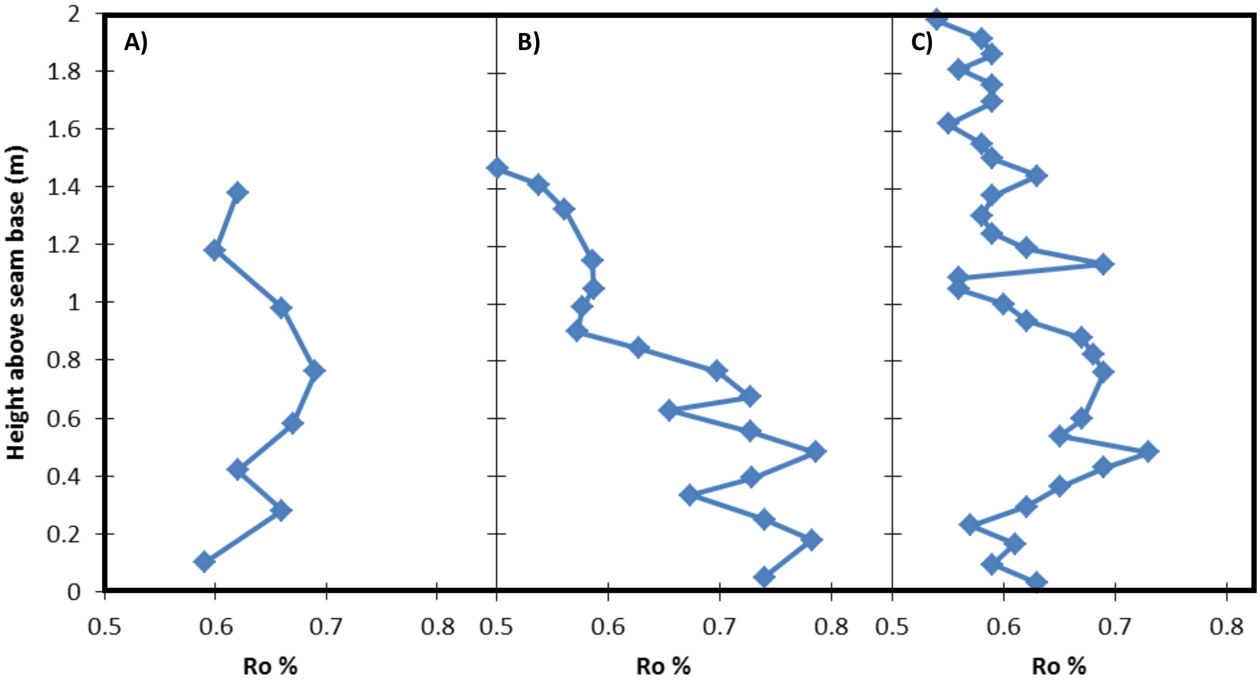

**Figure 4**

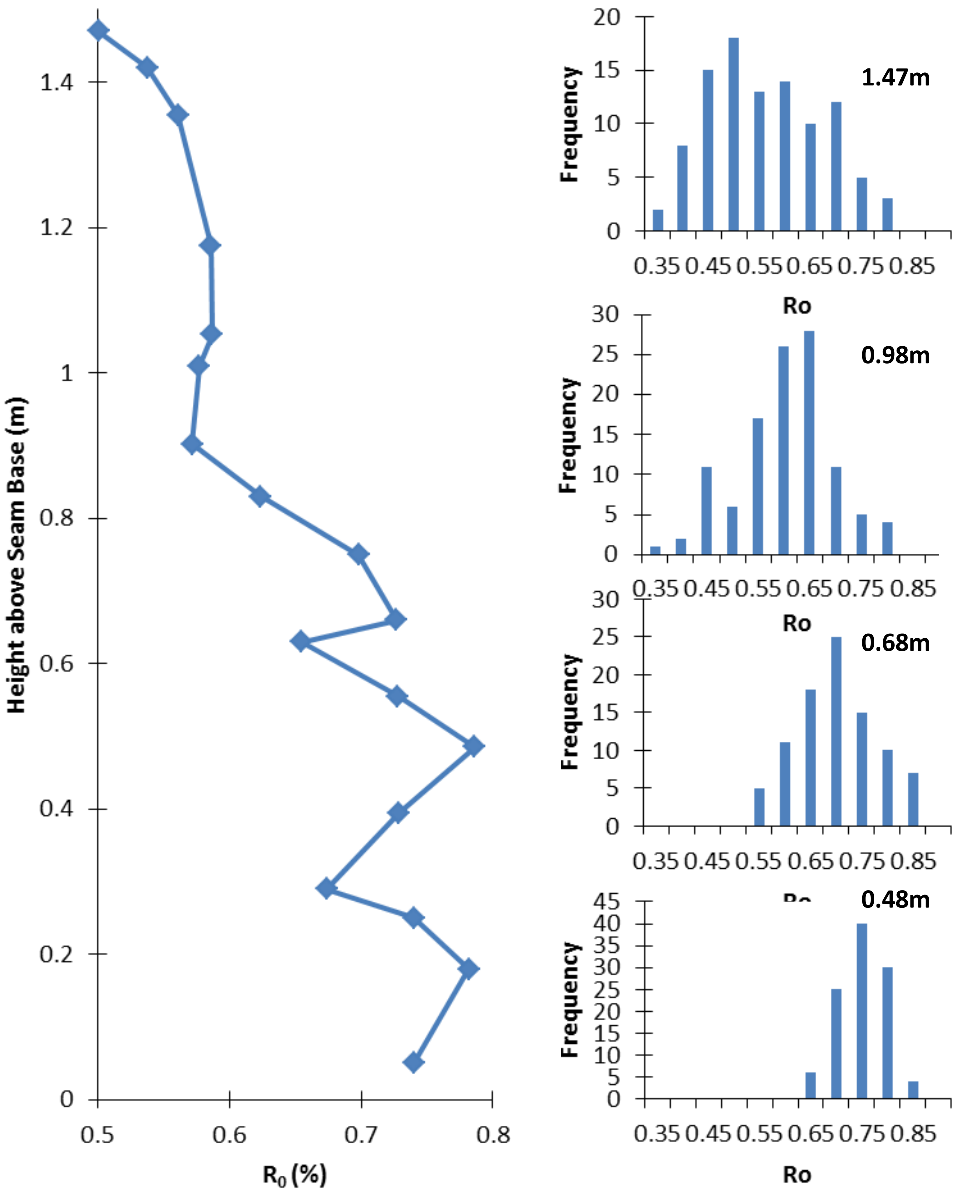

**Figure 5**

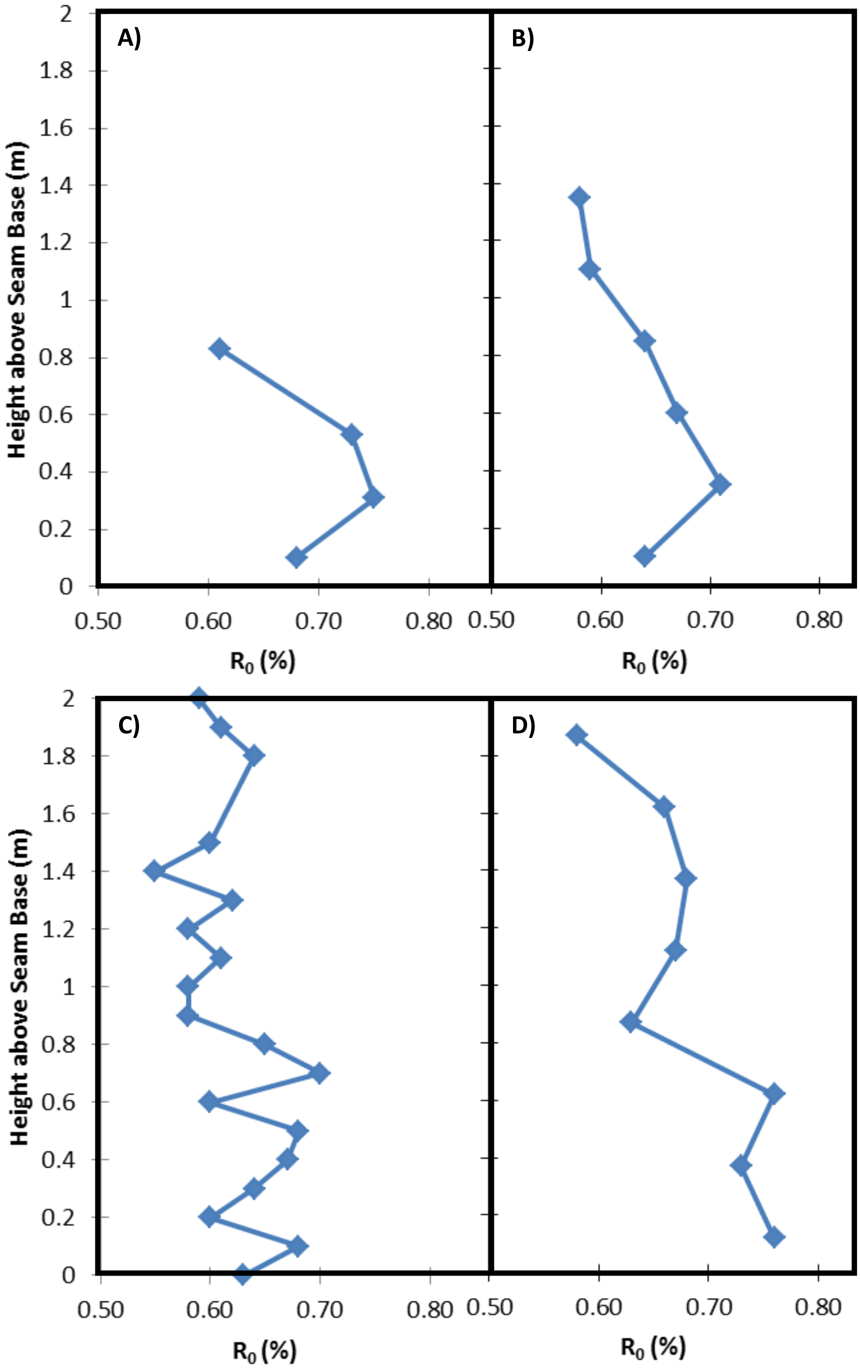
A)
B)
C)
D)
Height above Seam Base (m)
Height above Seam Base (m)
0
0.2
0.4
0.6
0.8
1
1.2
1.4
1.6
1.8
2
0.50
0.60
0.70
0.80
$R_0$ (%)
$R_0$ (%)
$R_0$ (%)
$R_0$ (%)

**Figure 6**

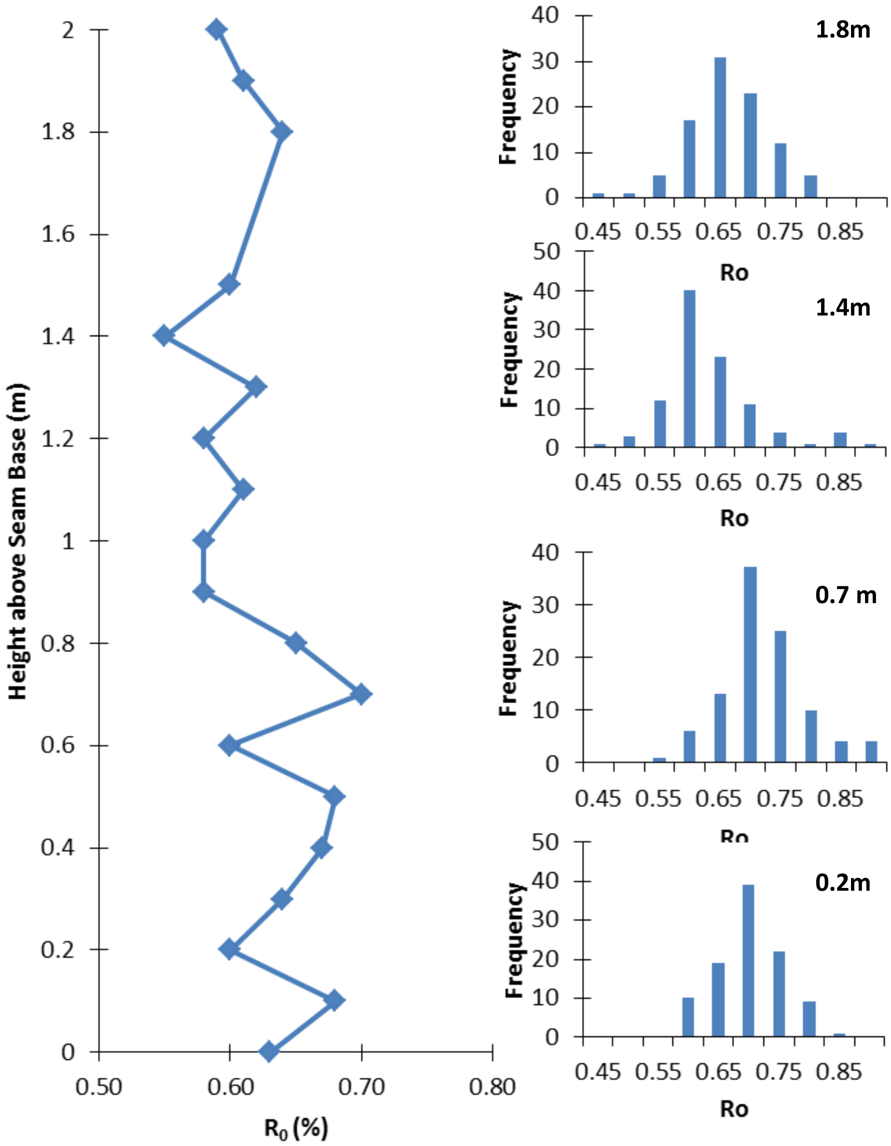
Height above Seam Base (m)
$R_0$ (%)
Frequency
Ro
1.8m
1.4m
0.7 m
0.2m
0.50
0.60
0.70
0.80
0.45 0.55 0.65 0.75 0.85

**Figure 7**

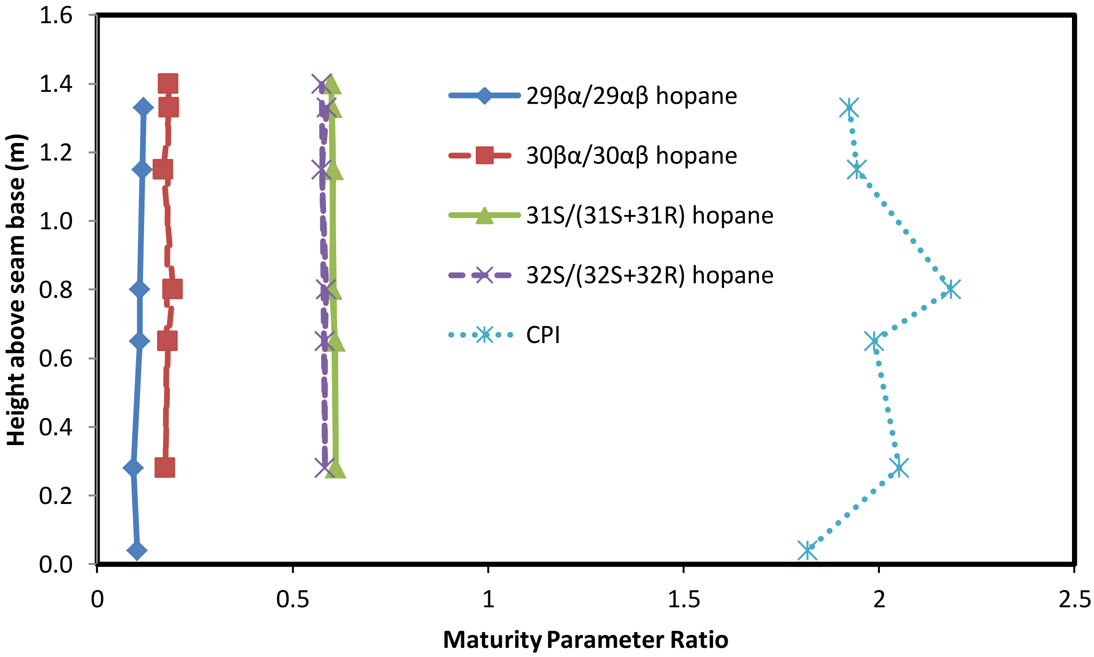

1.6
1.4
1.2
1.0
0.8
0.6
0.4
0.2
0.0
Height above seam base (m)
0
0.5
1
1.5
2
2.5
Maturity Parameter Ratio
29βα/29αβ hopane
30βα/30αβ hopane
31S/(31S+31R) hopane
32S/(32S+32R) hopane
CPI

**Figure 8**

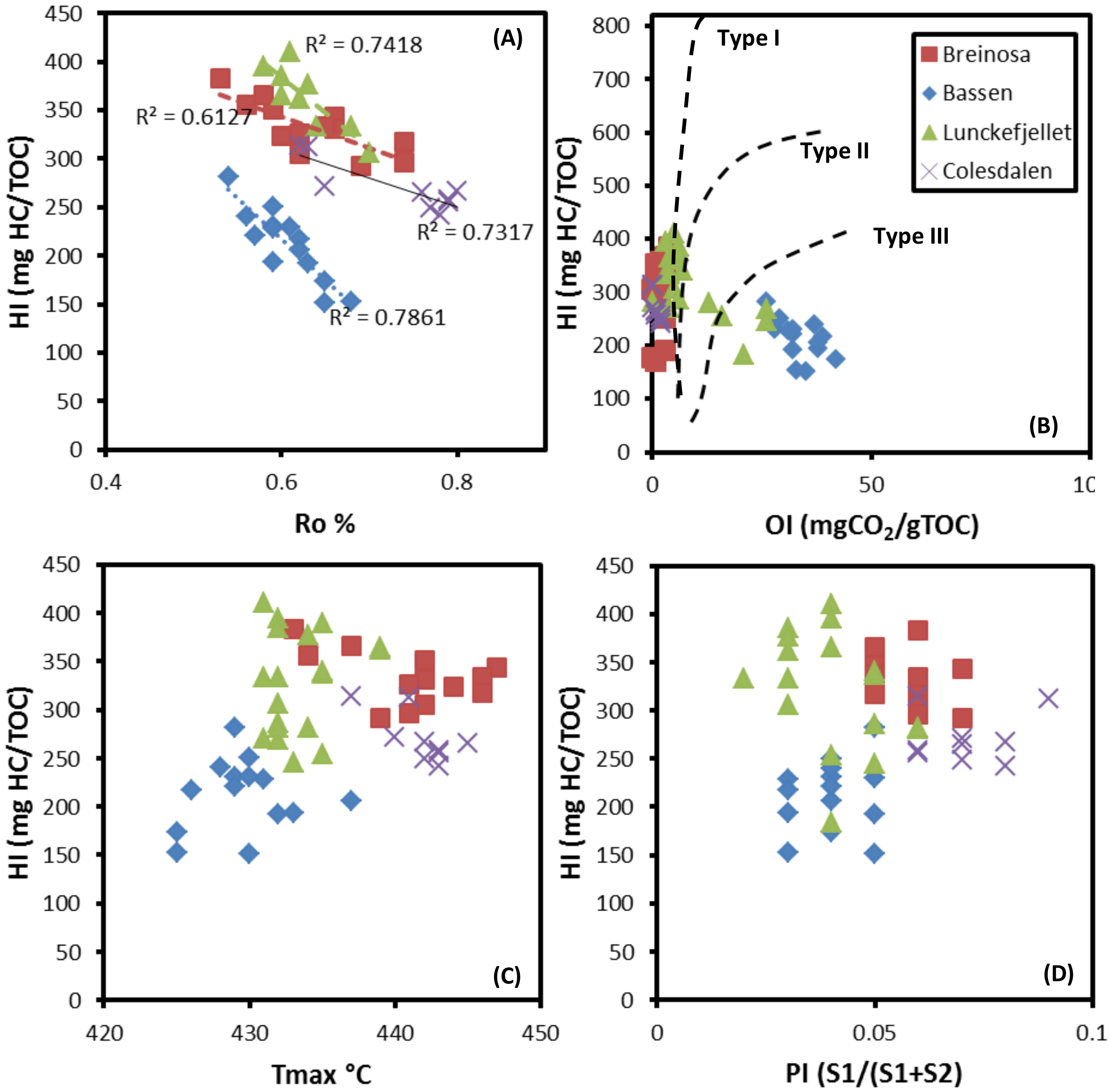
(A)
R² = 0.7418
R² = 0.6127
R² = 0.7317
R² = 0.7861
HI (mg HC/TOC)
Ro %
(B)
Type I
Type II
Type III
Breinosa
Bassen
Lunckefjellet
Colesdalen
HI (mg HC/TOC)
OI (mgCO2/gTOC)
(C)
HI (mg HC/TOC)
Tmax °C
(D)
HI (mg HC/TOC)
PI (S1/(S1+S2)

**Figure 9**

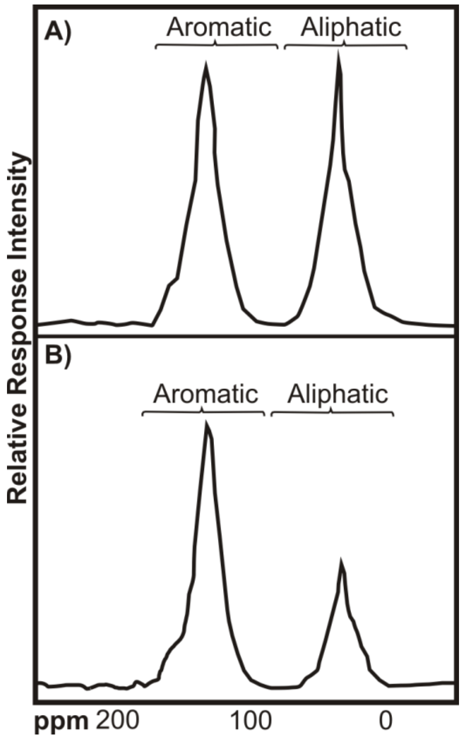
A)
Aromatic
Aliphatic
B)
Aromatic
Aliphatic
Relative Response Intensity
ppm 200
100
0

**Table 1**

| Seam | Seam Height (m) | $R_o$ | Pr/Ph | Pr/$nC_{17}$ | Ph/$nC_{18}$ | CPI(1) | Ts/Tm | $C_{29}$ βα/αβ | $C_{30}$ βα/αβ | $C_{31}$ S/(S+R) | $C_{32}$ S/(S+R) | $C_{33}$ S/(S+R) | $C_{29}/C_{30}$ αβ | $C_{35}/C_{34}$ αβ | C29 S/S+R | C29 β/α+β | TS/TH | MPI-1[a] | Calculated $R_o$[b] |
|---|---|---|---|---|---|---|---|---|---|---|---|---|---|---|---|---|---|---|---|
| | | | *n*-alkanes | | | | Hopanes | | | | | | | | Sterane | | | Aromatic | |
| Svea Nord | Bulk | 0.78 | 7.1 | 0.9 | 0.1 | 1.05 | 0.95 | 0.05 | 0.07 | 0.64 | 0.62 | 0.63 | 0.75 | 0.31 | 0.54 | 0.46 | 0.23 | 0.60 | 0.76 |
| Longyear | Bulk | 0.65 | 13.40 | 4.50 | 0.20 | 1.10 | 0.93 | 0.05 | 0.10 | 0.64 | 0.63 | 0.61 | 0.75 | 0.41 | 0.56 | 0.49 | 0.19 | 0.63 | 0.78 |
| Svea Nord | 0.07 | 0.77 | 4.48 | 24.55 | 4.43 | 1.46 | 0.93 | 0.09 | 0.08 | 0.58 | 0.58 | 0.58 | 0.58 | 0.43 | 0.42 | 0.51 | 0.21 | 0.48 | 0.69 |
| Svea Nord | 0.82 | 0.78 | 4.82 | 2.80 | 0.43 | 1.54 | 0.93 | 0.08 | 0.12 | 0.60 | 0.60 | 0.62 | 0.60 | 0.16 | 0.48 | 0.5 | 0.19 | 0.65 | 0.79 |
| Breinosa Svea | 0.75 | 0.78 | 3.51 | 22.48 | 3.77 | 1.41 | 0.94 | 0.07 | 0.09 | 0.59 | 0.59 | 0.62 | 0.63 | 0.23 | 0.51 | 0.51 | 0.19 | 0.51 | 0.71 |
| Breinosa Svea | 0.50 | 0.78 | 6.29 | 17.33 | 2.01 | 1.50 | 0.95 | 0.10 | 0.11 | 0.60 | 0.60 | 0.61 | 0.59 | 0.14 | 0.54 | 0.5 | 2 | 0.51 | 0.70 |
| Breinosa Svea | 1.00 | 0.79 | 3.53 | 2.70 | 0.66 | 1.54 | 0.93 | 0.08 | 0.09 | 0.62 | 0.62 | 0.64 | 0.56 | - | 0.47 | 0.53 | 0.2 | 0.49 | 0.69 |
| Breinosa Svea | 1.25 | 0.76 | 26.54 | 75.45 | 1.87 | 1.42 | 0.92 | 0.08 | 0.10 | 0.59 | 0.59 | 0.62 | 0.47 | 0.19 | 0.45 | 0.55 | 0.2 | 0.47 | 0.68 |
| Todalen | - | 0.75 | 20.99 | 119.83 | 2.93 | 1.39 | 0.93 | 0.06 | 0.07 | 0.60 | 0.60 | 0.63 | 0.55 | 0.28 | 0.47 | 0.49 | 0.21 | 0.57 | 0.74 |
| Svarteper | 0.73 | 0.65 | 3.01 | 0.68 | 0.27 | 1.40 | 0.91 | 0.10 | 0.05 | 0.58 | 0.58 | 0.59 | 0.50 | - | 0.48 | 0.52 | 0.2 | 0.76 | 0.86 |
| Svarteper | 0.94 | 0.65 | 6.49 | 9.99 | 0.97 | 1.57 | 0.95 | 0.09 | 0.13 | 0.60 | 0.60 | 0.61 | 0.61 | 0.16 | 0.49 | 0.51 | 0.21 | 0.56 | 0.74 |
| Askeladden | 0.33 | 0.64 | 2.95 | 6.23 | 1.73 | 1.39 | 0.94 | 0.11 | 0.10 | 0.59 | 0.59 | 0.62 | 0.54 | 0.29 | 0.48 | 0.5 | 0.21 | 0.52 | 0.71 |
| Longyear | 1.43 | 0.501 | 3.46 | 7.75 | 0.18 | 1.40 | 0.92 | 0.08 | 0.06 | 0.58 | 0.58 | 0.60 | 0.51 | 0.49 | 0.43 | 0.51 | 0.2 | 0.51 | 0.71 |
| Longyear | 1.43 | 0.538 | 11.44 | 12.22 | 1.34 | 1.59 | 0.93 | 0.11 | 0.07 | 0.60 | 0.59 | 0.60 | 0.67 | 0.30 | 0.45 | 0.49 | 0.18 | 0.51 | 0.71 |
| Longyear | 1.35 | 0.561 | 10.13 | 20.67 | 1.56 | 1.53 | 0.94 | 0.10 | 0.11 | 0.60 | 0.57 | 0.60 | 0.60 | 0.31 | 0.43 | 0.50 | 0.2 | 0.49 | 0.69 |
| Longyear | 1.17 | 0.586 | 11.41 | 17.37 | 1.15 | 1.56 | 0.95 | 0.09 | 0.12 | 0.60 | 0.59 | 0.62 | 0.62 | 0.30 | 0.45 | 0.50 | 0.21 | 0.55 | 0.73 |
| Longyear | 0.83 | 0.628 | 13.42 | 15.42 | 0.81 | 1.62 | 0.93 | 0.08 | 0.09 | 0.61 | 0.58 | 0.61 | 0.60 | 0.03 | 0.41 | 0.52 | 0.22 | 0.49 | 0.69 |
| Longyear | 0.66 | 0.655 | 12.11 | 5.29 | 0.33 | 1.69 | 0.93 | 0.08 | 0.10 | 0.61 | 0.58 | 0.60 | 0.62 | 0.41 | 0.41 | 0.52 | 0.23 | 0.55 | 0.73 |
| Longyear | 0.29 | 0.74 | 12.31 | 6.20 | 0.35 | 1.72 | 0.93 | 0.10 | 0.10 | 0.60 | 0.58 | 0.59 | 0.62 | 0.31 | 0.40 | 0.51 | 0.18 | 0.54 | 0.73 |
| Longyear | 0.07 | 0.74 | 13.60 | 2.34 | 0.16 | 1.69 | 0.94 | 0.11 | 0.12 | 0.60 | 0.57 | 0.61 | 0.63 | 0.31 | 0.42 | 0.51 | 0.19 | 0.45 | 0.67 |